

A Globally Optimal Bilinear Programming Approach to the Design of Approximate Hilbert Pairs of Orthonormal Wavelet Bases*

Jiang WANG and Jian Qiu ZHANG

State Key Laboratory of ASIC & System and Dept. of E. E., Fudan University, Shanghai, 200433, P. R. CHINA

Tel: +86-21-55664226, Fax: +86-21-55664226, e-mail: jqzhang@fudan.ac.cn

Abstract—It is understood that the Hilbert transform pairs of orthonormal wavelet bases can only be realized approximately by the scaling filters of conjugate quadrature filter (CQF) banks. In this paper, the approximate realization of the Hilbert transform pairs is first formatted as an optimization problem in the sense of the l_p ($p=1, 2$, or infinite) norm minimization on the magnitude and phase conditions of the scaling filters. The CQF bank conditions are taken as the constraints of such an optimization problem. Then a bilinear programming approach with the branch and bound technique is employed to obtain the globally optimal solution of the constrained optimization problem. Since the combined influences of the magnitude and phase conditions of the scaling filters on the approximation quality of the designed Hilbert transform pair are jointly and optimally taken into consideration, the attained solution is a better approximated Hilbert transform pair. Some orthogonal wavelet bases designed by us herein demonstrate that our design scheme is superior to those that have been reported in literatures.

Index Terms—Conjugate quadrature filter (CQF), dual-tree complex wavelet transform (DTWT), bilinear programming, Hilbert transform, orthonormal wavelet bases

I. INTRODUCTION

It is well known that the discrete wavelet transform (DWT) is a powerful signal processing tool. However, it has some disadvantages that undermine its usage in many applications. For example, one of the disadvantages is that the DWT is not a shift-invariant transform, which is undesirable in many pattern recognition applications [1]. Moreover, the poor directionality and lack of phase information of the DWT are also unfavorable in these applications. In order to overcome these disadvantages, Kingsbury's complex dual-tree wavelet transform (DTWT) has

been proposed in [2]. The complex DTWT is constructed by a (approximate) Hilbert pair of wavelets. It has been shown that the Hilbert pair construction is very crucial for making the complex DTWT be able to reduce the shift variance, improve the directionality, and provide the explicit phase information [3].

It has been proved in [4] that, in order to ensure the orthonormal wavelet bases as a Hilbert transform, its two lowpass conjugate quadrature filters (CQFs) should have the equal magnitude response and half-sample phase delay relationship, *i.e.*, $G(\omega)=H(\omega)e^{j(\omega/2)}$ for $\omega<\pi$, where $G(\omega)$ and $H(\omega)$ are the frequency responses of the two lowpass CQFs respectively. Therefore, designing a Hilbert pair for the complex DTWT is reduced to designing two lowpass CQFs whose frequency responses $G(\omega)$ and $H(\omega)$ satisfy such a relationship.

Several schemes for designing the desirable CQFs have been proposed in recent years. Selesnick has presented two design schemes. One is based on constructing the scaling filter pairs of the CQFs such that the required half-sample delay is approximately achieved near $\omega=0$ [4]. This design scheme cannot guarantee the required half-sample delay at frequencies far from $\omega=0$. Another is dependent on the design of an all-pass filter with an approximate constant fractional delay [5]. This scheme can design CQFs with good approximated half-sample delay property. However, the approximation quality of the designed CQFs is far from the optimality [6]. Tay has shown that two Daubechies wavelets whose length differs by four and vanishing moments differ by two form approximate Hilbert pairs [7]. He has also pointed out that the techniques based on joint approximation of the magnitude and phase conditions of the CQFs open up the possibility of constructing a much larger class of Hilbert pairs with better approximation quality. At the almost same time, Shi et. al. proposed a design scheme with separately optimal approximation to the magnitude and phase conditions of the CQFs [6]. Their scheme can design Hilbert pairs with better approximation but requires that the vanishing moments of the two CQFs differ by 1, which may be undesirable for some applications. Furthermore, their optimization approach is to locally optimize a non-convex optimization problem. As a result, the approximation performance of the designed Hilbert pairs

* This work was supported by the National Natural Science Foundation of China under Grant 60872058 and the National Key Basic Research Program (NKBRP) of China under Grant 2006CB705700.

heavily depends on the selection of the initial starting point of optimization.

Optimal filter design schemes have been widely used in designing both FIR and IIR filters [8] [9]. These design schemes can design filters by optimizing with respect to filter coefficients to satisfy the desired performance requirements. However, to the authors' knowledge, designing the required CQFs for DTWT with optimal filter design schemes has not been reported in literature. Here, we propose a novel approach that formats the construction of the equal magnitude responses and half-sample phase offset, $G(\omega)=H(\omega)e^{j(\omega/2)}$ for $\omega<\pi$, as the problem to make the frequency response error, $H(\omega)e^{j(\omega/2)}-G(\omega)$, minimized. That is to jointly approximate the magnitude and phase conditions of the two CQFs by minimizing the l_p ($p=1, 2$, or ∞) norm of the frequency response error. Such an objective function takes the interaction between the magnitude and phase response approximations of the CQFs into consideration. Thus, better approximation quality for the designed wavelets as Hilbert pairs can be expected. The resulting optimization problem is taken as a bilinear optimization one, where the branch and bound technique in [10] is employed to achieve the global optimal solution. Therefore, unlike design schemes that use local nonlinear optimization, our design scheme always produces consistent results. Moreover, our design scheme does not have any restriction on the designed Hilbert pairs. The design examples demonstrate that the approximation quality of the designed Hilbert pairs here is superior to those that have been reported in literatures. These examples also indicate that the best approximation results are got by minimizing the frequency response error's l_1 norm instead of by minimizing its l_2 or l_∞ norm.

The rest of this paper is organized as follows. Section II provides some preliminaries. Our design scheme is described in Section III. Some design examples and the approximation performance comparison with the designed Hilbert pairs in literatures are given in Section IV. Section V concludes this paper.

II. PRELIMINARY

A. Orthonormal Compactly Supported Wavelet Bases

Let the filters $h_0(n)$ and $h_1(n)$ represent a CQF pair [11]. That is

$$\sum_n h_0(n)h_0(n+2k) = \delta(k) = \begin{cases} 1, & k=0 \\ 0, & k \neq 0 \end{cases}$$

and $h_1(n) = (-1)^n h_0(L-n)$, where L is an odd integer, and the length of each filter is $L+1$. Equivalently in frequency domain, we have

$$|H_0(\omega)| + |H_0(\omega+\pi)| = 2. \quad (1)$$

Daubechies has shown in [12] that the trigonometric polynomial $H_0(\omega)$ of the form

$$H_0(\omega) = \left(\frac{1+e^{-i\omega}}{2}\right)^N q(\omega) \quad (2)$$

satisfies (1) if and only if $Q(\omega) = |q(\omega)|^2$ can be written as

$$Q(\omega) = P_N(y) + y^N R(0.5-y), \quad (3)$$

where $y = \sin^2(\omega/2)$, N is the vanishing moment of the designed wavelet,

$$P_N(y) = \sum_{k=0}^{N-1} \binom{N-1+k}{k} y^k,$$

and $R(\cdot)$ is an odd polynomial, chosen such that $P(y) \geq 0$ for all $y \in [0, 1]$.

Daubechies applies spectral factorization to construct $q(\omega)$ from $Q(\omega)$. However, since an optimal phase response of the $q(\omega)$ is expected in this paper, $q(\omega)$ should be dealt with directly. Accordingly, the explicit relationship between the $q(\omega)$ and $Q(\omega)$ is required and will be given in Section III.

B. Hilbert Transform pairs

In [4], it is shown that if $H_0(\omega)$ and $G_0(\omega)$ are two lowpass CQFs with

$$G_0(\omega) = H_0(\omega)e^{j(\frac{\omega}{2})} \text{ for } |\omega| < \pi, \quad (4)$$

then the corresponding wavelets form a Hilbert transform pair

$$\psi_g(t) = H[\psi_h(t)],$$

where

$$H[\psi_h(t)] = \begin{cases} -j\psi_h(t), & \omega > 0 \\ j\psi_h(t), & \omega < 0 \end{cases}.$$

III. DESIGN SCHEME

It has been understood that the equal magnitude response and half sample phase delay in (4) cannot be approached simultaneously [6]. Therefore, we can only design approximate Hilbert pairs. Based on (4), the design approximate error should have the following form,

$$E(\omega) = H_0(\omega)e^{j(\frac{\omega}{2})} - G_0(\omega) \text{ for } |\omega| < \pi, \quad (5)$$

where $H_0(\omega)$ and $G_0(\omega)$ respectively satisfy the CQF pair constraint condition (1).

It should be noticed that our objective function (5) is quite different from that in [6]. In order to see the difference, let us suppose that $H_0(\omega) = [A(\omega) + \Delta A(\omega)]e^{j[\theta(\omega) - \omega/2 + \Delta\theta(\omega)]}$ and $G_0(\omega) = A(\omega)e^{j\theta(\omega)}$, where $\Delta A(\omega)$ and $\Delta\theta(\omega)$ are respectively the magnitude and phase approximate errors of the CQFs. In [6], the objective function is $|H_0(\omega)| \approx |G_0(\omega)|$ and $\angle H_0(\omega) - \angle G_0(\omega) \approx \omega/2$. It implies that both the magnitude and phase responses of the CQFs, $H_0(\omega)$ and $G_0(\omega)$, are independently approximated with the small magnitude and phase errors $\Delta A(\omega)$ and $\Delta\theta(\omega)$. (5) can be rewritten as

$$\begin{aligned} E(\omega) &= [A(\omega) + \Delta A(\omega)]e^{j[\theta(\omega) + \Delta\theta(\omega)]} - A(\omega)e^{j\theta(\omega)} \\ &\approx [A(\omega) + \Delta A(\omega)][e^{j\theta(\omega)} + je^{j\theta(\omega)}\Delta\theta(\omega)] - A(\omega)e^{j\theta(\omega)} \\ &\approx \Delta A(\omega)e^{j\theta(\omega)} + jA(\omega)e^{j\theta(\omega)}\Delta\theta(\omega) \end{aligned} \quad (6)$$

where the phase error, $\Delta\theta(\omega)$, is assumed small, the first order Taylor series expansion is used to approximate $e^{j[\theta(\omega)+\Delta\theta(\omega)]}$, and the higher-order term, $je^{j\theta(\omega)}\Delta\theta(\omega)\Delta A(\omega)$, is ignored.

From (6), one can see that, the smaller the $A(\omega)$ is, the lesser influence the phase error $\Delta\theta(\omega)$ has on the error function $E(\omega)$. Furthermore, one can also find that the error function $E(\omega)$ is related with both $\Delta A(\omega)$ and $\Delta\theta(\omega)$. Obviously, it may not be a suitable and/or optimal way to make the magnitude and phase responses of $H_0(\omega)$ and $G_0(\omega)$ independently approximated as done in [7]. What follows, the minimization of $E(\omega)$, which jointly takes the magnitude and phase errors $\Delta A(\omega)$ and $\Delta\theta(\omega)$ into consideration as given by (5), will be described.

It is well known that it is desirable in many applications to design two orthogonal wavelets with the same vanishing moments in order to make them have the similar properties. As a result, we, herein, only consider designing the CQFs with the same vanishing moments and length. Certainly, since the proposed design scheme is quite general, it can be employed to design the CQFs with different vanishing moments and/or filter length after some simple modifications.

Suppose that the designed two CQFs are h_0 and g_0 respectively. Their vanishing moments, N , is the same. According to (2), the frequency response of the h_0 and g_0 can be respectively written as

$$\begin{aligned} H_0(\omega) &= \left(\frac{1+e^{-i\omega}}{2}\right)^N q_h(\omega) \\ G_0(\omega) &= \left(\frac{1+e^{-i\omega}}{2}\right)^N q_g(\omega) \end{aligned}, \quad (7)$$

where $H_0(\omega)$ and $G_0(\omega)$ are the frequency responses of h_0 and g_0 respectively.

Let the FIR filters with the frequency response $q_h(\omega)$ and $q_g(\omega)$ be $\mathbf{q}_h = [h(0), \dots, h(M-1)]^T$ and $\mathbf{q}_g = [g(0), \dots, g(M-1)]^T$ respectively. It means that the lengths of both the h_0 and g_0 are $M+N$.

A. CQF constraint

Let us first derive the constraint (1) on h_0 . Since h_0 and g_0 have the same vanishing moments and length, the constraint (1) on them are exactly the same. Therefore, we only give the constraint (1) on h_0 in this subsection, whereas the constraint (1) on g_0 can be derived by the same way.

From (3), it is known that $Q_h(\omega) = |q_h(\omega)|^2$ should have the form

$$Q_h(\omega) = \sum_{k=0}^{N-1} \binom{N-1+k}{k} y^k + y^N R_h(0.5-y), \quad (8)$$

where $y = \sin^2(\omega/2)$, N is the vanishing moment of the designed wavelet and R_h is an odd polynomial of degree $M-N-1$. Take $r=M-N-1$, where r is odd because $M+N$ is odd. Suppose

$$R_h(0.5-y) = \sum_{n=0}^{(r-1)/2} a_n (0.5-y)^{2n+1}. \quad \text{By Binomial theorem, we}$$

have

$$R_h(0.5-y) = \sum_{k=0}^r y^k \sum_{n=0}^{\lfloor (k-1)/2 \rfloor} \binom{2n+1}{k} 0.5^{2n+1-k} a_n, \quad (9)$$

where $\lfloor x \rfloor$ represents the largest integer smaller than x .

Suppose

$$Q(\omega) = \sum_{k=0}^{M-1} c_k y^k. \quad (10)$$

By comparing (10) with (9) and (8), we have

$$c_k = \begin{cases} \binom{N-1+k}{k} & k < N \\ \sum_{n=0}^{\lfloor (k-N-1)/2 \rfloor} \binom{2n+1}{k} 0.5^{2n+1-k} a_n & N \leq k < M \end{cases}. \quad (11)$$

The constraint (1) on Q_h is thus (11).

Then we will derive the relationship between Q_h and q_h . In terms of Z-transform, one has

$$Q_h(z) = q_h(z)q_h(z^{-1}). \quad (12)$$

Let $Q_h(z) = \sum_{k=-M-1}^{M-1} \eta(k)z^{-k}$ and $q_h(z) = \sum_{k=0}^{M-1} h(k)z^{-k}$. Based

on (12), the relationship between $\eta(k)$, the impulse response of Q_h , and $h(k)$, the impulse response of q_h , can be written as

$$\eta(k) = \sum_{m-n=|k|} h(m)h(n). \quad (13)$$

(13) is the relationship between $\eta(k)$ and h_k .

Finally, the relationship between $\eta(k)$ and c_k will be derived. Substituting

$$y = \sin^2(\omega) = \frac{1-(e^{j\omega} + e^{-j\omega})/2}{2} = \frac{1-(z+z^{-1})/2}{2}$$

into (10), Q_h can be rewritten as

$$Q_h(z) = \sum_{k=0}^{M-1} c_k \left(\frac{1-(z+z^{-1})/2}{2}\right)^k. \quad (14)$$

Suppose

$$\left(\frac{1-(z+z^{-1})/2}{2}\right)^k = \sum_{n=-k}^k t_n^k z^n. \quad (15)$$

By applying Binomial theorem twice, we can get

$$t_n^k = t_{-n}^k = \begin{cases} \sum_{n \leq m \leq k, m \text{ is even}} \left(-\frac{1}{2}\right)^m \binom{k}{m} \binom{m}{\frac{m-n}{2}}, & n \text{ is even} \\ \sum_{n \leq m \leq k, m \text{ is odd}} \left(-\frac{1}{2}\right)^m \binom{k}{m} \binom{m}{\frac{m-n}{2}}, & n \text{ is odd} \end{cases}. \quad (16)$$

(16) shows that t_n^k in (15) is a constant only depending on k and n .

Insert (15) into (14) and consider that $Q_h(z) = \sum_{k=-M-1}^{M-1} \eta(k)z^{-k}$, one can get

$$\eta(m) = \sum_{k=m}^{M-1} t_m^k c_k. \quad (17)$$

The analyses as above show that the constraint (1) on h_0 can be expressed as (11), (13), and (17), where the constraint (1) on Q_h is (11), the association between the impulse responses $\eta(m)$ of Q_h and $h(k)$ of q_h is (13), and the relationship between $\eta(m)$ and c_k is (17).

B. Half sample delay joint approximation

The half sample delay constraint of a Hilbert transform pair cannot be exactly realized as discussed in [6]. The techniques based on joint approximation of the magnitude and phase conditions of the half sample delay constraint to construct a much larger class of Hilbert pairs with better approximation quality are appealed in [5]. In order to respond such an appeal, one can obviously take (5) as an objective function to minimize due to the fact that the magnitude and phase conditions of the half sample delay constraint are jointly included in (5). How to minimize (5) across all frequencies with respect to the coefficients of the filters \mathbf{q}_h and \mathbf{q}_g will be given as followings.

By substituting (7) into (5), $E(\omega)$ can be rewritten as

$$E(\omega) = \left(\frac{1+e^{-i\omega}}{2} \right)^N [q_h(\omega)e^{j(\omega/2)} - q_g(\omega)]. \quad (18)$$

It is very difficult to minimize (18) directly because it is a continuous frequency response. A common practice is to first discretize it by frequency sampling as done in [13] and then to minimize it in the discrete domain. The frequency sampling is a technique sampling the frequency response function at some fixed points such as $-\pi \leq \omega_1 < \dots < \omega_m < \pi$. In this way, the minimization of (18) is equivalent to minimizing the norm of the error function $E(\omega)$ at these discrete frequency sampling points. Obviously, the more the sampling points, the better the samples reflect the frequency response across all the frequencies. However, the more the sampling points, the larger the computing burden is. Thus, the number of the sample points is usually chosen empirically as about 15 times of the filter length.

Let $q_h^r(\omega_k), q_h^i(\omega_k), q_g^r(\omega_k)$ and $q_g^i(\omega_k)$ be the real and imaginary parts of the $q_h(\omega_k)$ and $q_g(\omega_k)$ respectively, where $\omega_k = k\pi/T (k=-T, \dots, T)$ with T much larger than M , the length of \mathbf{q}_h , is the discrete frequency sampling point. Their discrete Fourier transform can be expressed as

$$\begin{aligned} [q_h^r(\omega_k), q_h^i(\omega_k)]^T &= \mathbf{A}^{(k)} \mathbf{q}_h \\ [q_g^r(\omega_k), q_g^i(\omega_k)]^T &= \mathbf{A}^{(k)} \mathbf{q}_g \end{aligned}, \quad (19)$$

where $\omega_k = k\pi/T (k=-T, \dots, T)$ and

$$\mathbf{A}^{(k)} = \begin{bmatrix} 1 & \cos(\omega_k) & \dots & \cos((M-1)\omega_k) \\ 0 & -\sin(\omega_k) & \dots & -\sin((M-1)\omega_k) \end{bmatrix}. \quad (20)$$

Let $E(\omega_k) = E^r(\omega_k) + jE^i(\omega_k)$. It can be easily seen from (18) and (19) that the relationship between $E^r(\omega_k), E^i(\omega_k)$ and $\mathbf{q}_h, \mathbf{q}_g$ is linear.

Let the vector \mathbf{e} defined as

$$\mathbf{e} = [E^r(\omega_{-T}), E^i(\omega_{-T}), \dots, E^r(\omega_T), E^i(\omega_T)], \quad (21)$$

where the elements of \mathbf{e} are the real and imaginary parts of the samples of the error function (18). In order to achieve the optimal approximation of the half sample delay of the two CQFs in the sense of l_p ($p=1, 2, \text{ or } \infty$) norm, minimizing $\|\mathbf{e}\|_p$ is required.

C. Optimization formula

In the previous subsections, we have derived the constraints that the h_0 and g_0 should satisfy to form the CQFs. The objective function able to be optimized to ensure the designed wavelet bases as an optimal approximate Hilbert pairs in the sense of the l_p norm has also been developed. In this way, an optimization-based approach in the sense of l_p norm to design pairs of dyadic wavelets bases forming an approximate Hilbert transform pair can be formatted as follows:

$$\min: \|\mathbf{e}\|_p$$

s.t.: constraints (11), (13) and (17) on

$$h_0 \text{ and } g_0 \text{ respectively.} \quad (22)$$

where \mathbf{e} is defined by (21). Notice that (11), (17) and (21) are linear with respect to the designed filter h_0 and g_0 coefficients, whereas there are the bilinear terms in (13). Meanwhile, the minimization of $\|\mathbf{e}\|_p$ in the sense of the l_p norm is an optimization problem that can be efficiently solved by the state of art of the optimization algorithms as those given in [14] when $p=1, 2, \text{ or } \infty$.

For example, minimizing $\|\mathbf{e}\|_2$ can be converted into the following second order cone programming (SOCP) problem [14]

$$\begin{aligned} \min: u \\ \text{s.t.: } \|\mathbf{e}\|_2 \leq u \end{aligned} \quad (23)$$

The $\|\mathbf{e}\|_\infty$ minimization can be solved via the following problem linear programming (LP) [14]

$$\begin{aligned} \min: u \\ \text{s.t.: } -u\mathbf{1} \leq \mathbf{e} \leq u\mathbf{1} \end{aligned} \quad (24)$$

where \leq denotes element-wise inequity, and $\mathbf{1}$ is a all 1 vector.

Similarly, the $\|\mathbf{e}\|_1$ minimization can also be got as following an LP [14]

$$\begin{aligned} \min: \mathbf{1}\mathbf{u} \\ \text{s.t.: } -\mathbf{u} \leq \mathbf{e} \leq \mathbf{u} \end{aligned} \quad (25)$$

As a result, if one wants to minimize the l_2 norm of (22), the optimization problem (22) is converted to

$$\min: u$$

$$\text{s.t.: } \|\mathbf{e}\|_2 \leq u$$

constraints (11), (13) and (17) on

h_0 and g_0 respectively,

$$(26)$$

where \mathbf{e} is defined by (21).

If $p=\infty$, the optimization problem (22) becomes

$$\begin{aligned} \min: & \mathbf{u} \\ \text{s.t.}: & -\mathbf{u}\mathbf{1} \leq \mathbf{e} \leq \mathbf{u}\mathbf{1} \\ & \text{constraints (11), (13) and (17) on} \\ & h_0 \text{ and } g_0 \text{ respectively,} \end{aligned} \quad (27)$$

where \leq denotes element-wise inequity, $\mathbf{1}$ is a all 1 vector, and \mathbf{e} is defined by (21).

If $p=1$, we can convert (22) to

$$\begin{aligned} \min: & \mathbf{1}\mathbf{u} \\ \text{s.t.}: & -\mathbf{u} \leq \mathbf{e} \leq \mathbf{u} \\ & \text{constraints (11), (13) and (17) on} \\ & h_0 \text{ and } g_0 \text{ respectively,} \end{aligned} \quad (28)$$

where \leq denotes element-wise inequity, $\mathbf{1}$ is a all 1 vector, and \mathbf{e} is defined by (21).

Since all of (26), (27) and (28) only include bilinear terms as their non-convexity, they are non-convex optimization problems called bilinear programming problem. Obviously, one cannot obtain their global optimal solutions by the conventional local optimization techniques. In the next subsection, How to obtain their globally optimal solutions with the branch and bound technique in [17] is discussed and shown.

D. Solving optimization

Bilinear programming has been widely explored in the optimization community. However, most existing algorithms either require the bilinear programming to be disjoint [15] or have no guarantee on the convergence to the global optimal solution [16]. In order to achieve the global optimal solution for our bilinear programming problems (26), (27) and (28), the branch and bound algorithm in [17] is improved to fit our problems. The main difference between our problem and that in [17] is that our local nonlinear optimization in some points could be infeasible. Thus, the upper bound used in this paper is different from that in [17].

The branch and bound algorithms contain two parts. One is to find a lower and an upper bound of the given problem in a region. Another is to devise a branching strategy to decide which region should be split and bounded to achieve tighter global bounds. By iteratively refining the global lower and upper bounds of the optimization problem by branching, the provable global ε -suboptimal solution can be obtained when the difference between the global lower and upper bounds is less than ε . If ε is small, the obtained solution can be considered global optimal [6].

The upper bounds of (26), (27), and (28) in a given region can be obtained by local nonlinear optimization with a randomly chosen initial point in such region. However it is possible that the local nonlinear optimization with such a randomly selecting initial point is infeasible. If it happens, one should try to start the optimization with another randomly initial point in this region. Otherwise one may set the upper bound into ∞ if such a case continually occurs, e.g., say up to 5 times.

The lower bound is obtained by the same way as that in [17]. Namely, the bilinear term xy in domain $[x_l, x_u] \times [y_l, y_u]$ can be bounded by the following equation

$$\begin{aligned} xy & \geq \max\{x_l y + y_l x - x_l y_l, x_u y + y_u x - x_u y_u\} \\ xy & \leq \min\{x_u y + y_l x - x_u y_l, x_l y + y_u x - x_l y_u\} \end{aligned} \quad (29)$$

(29) can both be transformed into the following inequities

$$\begin{aligned} xy & \geq x_l y + y_l x - x_l y_l, xy \geq x_u y + y_u x - x_u y_u \\ xy & \leq x_u y + y_l x - x_u y_l, xy \leq x_l y + y_u x - x_l y_u \end{aligned} \quad (30)$$

It should be emphasized that the inequities in (30) is linear because the boundaries, x_b , x_u , y_b , and y_u of the domain $[x_l, x_u] \times [y_l, y_u]$ are known. By inserting (30) into (13) in (26), (27), and (28) respectively, (27) and (28) are relaxed into the linear programming problems, which can be conveniently solved by the simplex algorithm or the interior point algorithm [14], while (26) is relaxed into a second order cone programming problem that can also be efficiently solved. The lower bound of such a region can thus be attained by solving the corresponding relaxed problem.

Our branching strategy is to choose the region with the smallest lower bound and then the longest edge of this region corresponding to a variable in the bilinear terms is bisected. Let γ_k^l and γ_k^h be the global lower and upper bounds respectively. \mathcal{P}_k is the set of the regions at iteration k . D_0 is the domain of the optimization problem (26), (27) or (28). $\phi_{lb}(D)$ and $\phi_{ub}(D)$ are the upper and lower bounds of the region D respectively. In that way, our optimal algorithm can be summarized as follows:

- Set $k=0$, $\mathcal{P}_0 = \{D_0\}$
- while $\gamma_k^h - \gamma_k^l > \varepsilon$
 - ◆ choose $D \in \mathcal{P}_k$ such that $\phi_{lb}(D) = \gamma_k^l$
 - ◆ bisect the longest edge of D that corresponds only to some bilinear variables to form two rectangular D_1 and D_2 .
 - ◆ $\mathcal{P}_{k+1} = \{\mathcal{P}_k \setminus D\} \cup \{D_1, D_2\}$
 - ◆ solve $\phi_{ub}(D_1)$, $\phi_{ub}(D_2)$, $\phi_{lb}(D_1)$ and $\phi_{lb}(D_2)$
 - ◆ $\gamma_{k+1}^h = \min\{\gamma_k^h, \phi_{ub}(D_1), \phi_{ub}(D_2)\}$
 - ◆ $\gamma_{k+1}^l = \min\{\gamma_k^l, \phi_{lb}(D_1), \phi_{lb}(D_2)\}$
 - ◆ $k=k+1$

IV. DESIGN EXAMPLES

In our design examples, the number of sampling points of frequency sampling is 50. Each coefficient in \mathbf{q}_h and \mathbf{q}_g is bounded in $[-3, 3]$.

A scaling filter pair with length 8 and vanishing moment 2 is first designed by the approach in this paper with l_1 norm minimization. Table I tabulates the designed filter coefficients. Their magnitude responses, $|G_0(\omega)|$ and $|H_0(\omega)|$, and the phase offset $\theta(\omega)$ are illustrated in Fig. 1. It can be observed from the Fig. 1 that the magnitude responses of the filter pair

$|G_0(\omega)|$ and $|H_0(\omega)|$ are nearly equal, while their phase shift $\theta(\omega)$ is very close $\omega/2$ except near frequency $\omega = \pi$. Because the magnitude responses near frequency $\omega = \pi$ are very small, the phase shift errors near frequency $\omega = \pi$ do not have much effect on the overall approximation performance of the designed wavelet bases.

Let $|e_1|$ denote the magnitude response of the error function of our wavelet pair in Table I designed in the sense of the l_1 norm minimization and $|e_s|$ represent that of Shi *et. al.* wavelet pair (refer to the Table I of [6]). From Fig. 2. It can be seen that the $|e_1|$ is smaller than the $|e_s|$ across all the frequency and much smaller than the $|e_s|$ at low frequencies. As stated in Section III, the magnitude responses of the scaling filters are large at low frequencies and small at high frequencies. Fig. 2 shows that our design scheme weights the phase response errors at low frequencies more than those at high frequencies in order to make the error function (5) nearly equal across all the frequencies. However the design scheme in [6] independently minimizes the magnitude and phase response errors without taking the interaction between the phase and magnitude responses into consideration. In this way, the scaling filter pairs designed in [6] have small errors at low frequencies but large ones at high frequencies. This is why the approximation quality to Hilbert pair of scaling filter pairs designed in [6] is worse than the pairs designed here.

Two scaling filter pairs with length 8 and vanishing moment 2 are designed by (26) and (27) respectively. That is to respectively approach the design optimization in the sense of the l_∞ and l_2 norm minimizations. The designed filter coefficients are tabulated respectively in Table II and III. Let $|e_\infty|$, $|e_2|$, and $|e_1|$ respectively denote the magnitude response error functions in the sense of the l_∞ , l_2 , and l_1 norm minimizations. It can be seen from Fig. 3 that the maximum values of the $|e_1|$ and $|e_\infty|$ are nearly the same. However, $|e_1|$ is much smaller than $|e_\infty|$ except at a narrow high frequency band. It can also be found that the $|e_2|$ is much larger than the $|e_1|$ and $|e_\infty|$. In many applications, such as image processing [18], machine learning [19] and pattern recognition [20], it is found that the better results are obtained when an objective function is optimized by the l_1 norm minimization instead of the l_2 and l_∞ norm ones. Our applications as above also verify such a case. Consequently, it is recommended to design the wavelet bases approximated as a Hilbert pair by minimizing the error function (5) in the sense of the l_1 norm.

Other 3 scaling filter pairs are designed with our scheme by l_1 norm minimization. The filter coefficients of these filters are tabulated in Table IV, Table V, and Table VI respectively. The length of first filter is 10 and its vanishing moment is 3. The second filter is of length 12 and vanishing moment 4. The last filter is also of length 12, but its vanishing moment is 3.

If a pair of wavelets $(\psi^h(t), \psi^g(t))$ with the frequency response $(\Psi_h(\omega), \Psi_g(\omega))$ is related through the Hilbert transform. Tay *et. al.* propose the following two measures, E_1 (L^∞ measure) and E_2 (L^2 measure) in [21], to evaluate the approximation quality of the pair of wavelet bases as a Hilbert transform pair,

$$E_1 = \frac{\max_{\omega < 0} |\Psi_h(\omega) + i\Psi_g(\omega)|}{\max_{\omega > 0} |\Psi_h(\omega) + i\Psi_g(\omega)|}$$

$$E_2 = \frac{\int_{-\infty}^0 |\Psi_h(\omega) + i\Psi_g(\omega)|^2 d\omega}{\int_0^{\infty} |\Psi_h(\omega) + i\Psi_g(\omega)|^2 d\omega}$$

These two measures are also employed as the criteria to evaluate the wavelet bases we design and those in [4], [5] and [6]. Cascade algorithm with 10 levels is utilized to create the wavelet function. The results are tabulated in Table VII, where the wavelet bases designed in this paper are listed in bold. It can be seen from Table VII that the wavelet bases designed by us have the best approximation quality. Table VII also shows that the approximation quality of the wavelet bases designed by minimizing the l_1 norm of the error function (5) is much better than that by minimizing its l_∞ and l_2 norm.

V. CONCLUSIONS

In this paper, a novel scheme for designing the approximate Hilbert pairs of orthonormal wavelet bases has been proposed. In our scheme, the magnitude and phase conditions of the scaling filters of the CQF banks are jointly taken as the objective function of an optimization problem. The condition of the CQF banks is taken as the constraint of such an optimization problem. The objective function takes the combined influences of the magnitude and phase conditions of the scaling filters on approximation quality of the designed wavelet pair to the Hilbert transform pair into consideration. It can, therefore, better reflect the approximation quality of the designed wavelet pair. The branch and bound technique, which can guarantee a globally optimal solution, is employed to solve our non-convex optimization problem. Therefore, the optimization result of our scheme does not depend on the initial starting point chosen and is always consistent. The superiority of our design scheme over those reported in literatures is demonstrated by two commonly applied evaluation criteria. Furthermore, it is found that the minimization of the l_1 norm version of our constrained optimization problem yields the best approximation performance.

ACKNOWLEDGMENT

The authors will appreciate the stimulating and helpful discussions with Dr. Hongli Shi and Dr. David Tay.

REFERENCES

- [1] E.P. Simoncelli, W.T. Freeman, E.H. Adelson, and D.J. Heeger, "Shiftable multiscale transforms," *IEEE Transactions on Information Theory*, vol. 38, pp. 587-607, 1992.
- [2] N. Kingsbury, "Image processing with complex wavelets," *Philosophical Transactions of the Royal Society A: Mathematical, Physical and Engineering Sciences*, vol. 357, pp. 2543-2560, 1999.
- [3] F.C.A. Fernandes, I.W. Selesnick, R.L.C. van Spaendonck, and C.S. Burrus, "Complex wavelet transforms with allpass filters," *Signal Processing*, vol. 83, pp. 1689-1706, 2003.
- [4] I.W. Selesnick, "Hilbert transform pairs of wavelet bases," *IEEE Signal Processing Letters*, vol. 8, pp. 170-173, 2001.
- [5] I.W. Selesnick, "The design of approximate Hilbert transform pairs of wavelet bases," *Signal Processing, IEEE Transactions on*, vol. 50, pp. 1144-1152, 2002.
- [6] H. Shi, B. Hu, and J.Q. Zhang, "A Novel Scheme for the Design of Approximate Hilbert Transform Pairs of Orthonormal Wavelet Bases," *Signal Processing, IEEE Transactions on*, vol. 56, pp. 2289-2297, 2008.
- [7] D.B.H. Tay, "Daubechies Wavelets as Approximate Hilbert-Pairs?," *IEEE Signal Processing Letters*, vol. 15, pp. 57-60, 2008.
- [8] W.S. Lu, "Design of nonlinear-phase FIR digital filters: a semidefiniteprogramming approach," *Circuits and Systems, 1999. ISCAS'99. Proceedings of the 1999 IEEE International Symposium on*, 1999.
- [9] D. Gorinevsky and S. Boyd, "Optimization-Based Design and Implementation of Multidimensional Zero-Phase IIR Filters," *Circuits and Systems I: Regular Papers, IEEE Transactions on*, vol. 53, pp. 372-383, 2006.
- [10] E.L. Lawler and D.E. Wood, "Branch-And-Bound Methods: A Survey," *Operations Research*, vol. 14, pp. 699-719, 1966.
- [11] S. Mallat, *A Wavelet Tour of Signal Processing*, Academic Press, 1999.
- [12] I. Daubechies, "Orthonormal bases of compactly supported wavelets," *Comm. Pure Appl. Math.*, vol. 41, pp. 909-996, 1988.
- [13] W.R. Lee, L. Caccetta, K.L. Teo, and V. Rehbock, "Optimal design of complex FIR filters with arbitrary magnitude and group delay responses," *Signal Processing, IEEE Transactions on*, vol. 54, pp. 1617-1628, 2006.
- [14] S.P. Boyd and L. Vandenberghe, *Convex Optimization*, Cambridge University Press, 2004.
- [15] D.J. White, "A linear programming approach to solving bilinear programmes," *Mathematical Programming: Series A and B*, vol. 56, pp. 45-50, 1992.
- [16] H. Konno, "A cutting plane algorithm for solving bilinear programs," *Mathematical Programming*, vol. 11, pp. 14-27, 1976.
- [17] M. Chandraker and D. Kriegman, "Globally Optimal Bilinear Programming for Computer Vision Applications," *Computer Vision and Pattern Recognition, 2008. CVPR 2008. IEEE Conference on*, 2008, pp. 1-8.
- [18] J. Yang, J. Wright, T. Huang, and Y. Ma, "Image super-resolution as sparse representation of raw image patches," *Proc. IEEE Conference on Computer Vision and Pattern Recognition*, 2008.
- [19] R. TIBSHIRANI, "Regression shrinkage and selection via the lasso," *Journal of the Royal Statistical Society. Series B. Methodological*, vol. 58, pp. 267-288, 1996.
- [20] J. Wright, A.Y. Yang, A. Ganesh, S.S. Sastry, and Y. Ma, "Robust Face Recognition via Sparse Representation," *Pattern Analysis and Machine Intelligence, IEEE Transactions on*, vol. 31, pp. 210-227, 2009.
- [21] D.B.H. Tay, N.G. Kingsbury, and M. Palaniswami, "Orthonormal Hilbert-Pair of Wavelets With (Almost) Maximum Vanishing

Moments," *Signal Processing Letters, IEEE*, vol. 13, pp. 533-536, 2006.

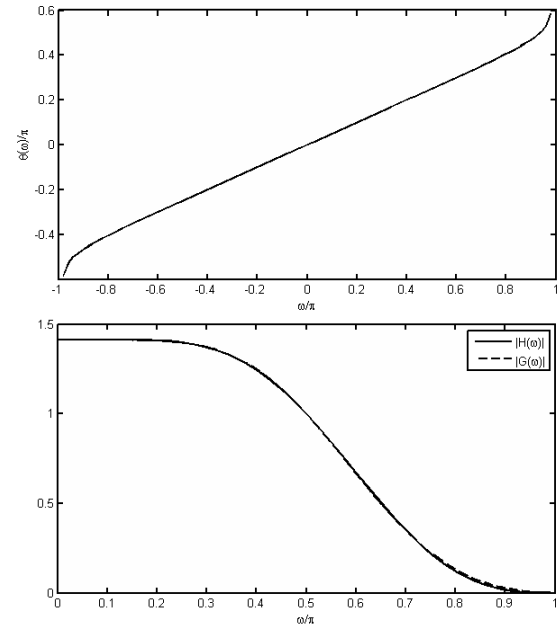


Fig. 1. $\theta(x)$ is phase offset, and $|H(\omega)|$ and $|G(\omega)|$ are respectively the magnitude responses of the two scaling filters in Table I.

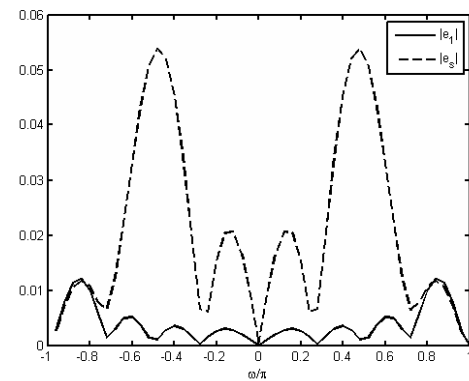


Fig. 2. e_1 is the error function of our wavelet pair in Table I, and e_s is the error function of the wavelet pair in Table I in [6].

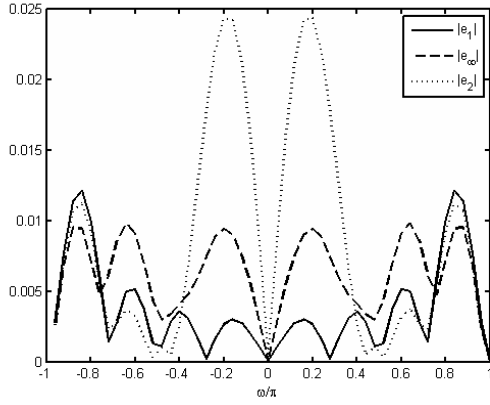


Fig. 3. e_1 is the error function of our wavelet pair in Table I designed by l_1 norm, while e_∞ is the error function of our wavelet pair in Table II, designed by l_∞ norm and e_2 is the error function of our wavelet pair in Table III designed by l_2 norm.

TABLE I

FILTER COEFFICIENTS WITH LENGTH 8 AND VANISHING MOMENT 2 DESIGNED BY l_1 NORM

h_0	g_0
-0.00427959286786331	-0.00499789193762367
0.044171008982978	0.019187661828230
-0.0630382813630226	0.026308453148234
-0.187282514910405	-0.174635809332290
0.352664111817497	0.001414777458855
0.809354163953011	0.684300031715614
0.421760543599936	0.684381442517082
0.040864123160963	0.178254896974993

TABLE II

FILTER COEFFICIENTS WITH LENGTH 8 AND VANISHING MOMENT 2 DESIGNED BY l_∞ NORM

h_0	g_0
0.227160307638364	0.0618374780870480
0.734065609480335	0.487642510575487
0.618016255787673	0.804531208889083
-0.0587534404167462	0.261874031694562
-0.150679923188365	-0.198843772960451
0.0356969542878341	-0.0373911254434504
0.0126101409488755	0.0395818671708672
-0.00390234216487549	-0.00501863564005050

TABLE III

FILTER COEFFICIENTS WITH LENGTH 8 AND VANISHING MOMENT 2 DESIGNED BY l_2 NORM

h_0	g_0
-0.0577494199391096	-0.0285743106243928
0.113358418339598	-0.0410402363109904
0.693720956105754	0.391384397749186
0.697631734865556	0.829191501052854
0.0559947553429332	0.379263182559141
-0.111596926419519	-0.105399856395129
0.0151404896769704	-0.0349664884973866
0.00771355440091325	0.0243553728398125

TABLE IV

FILTER COEFFICIENTS WITH LENGTH 10 AND VANISHING MOMENT 3 DESIGNED BY l_1 NORM

h_0	g_0
0.011345021299679	0.004986233899958
-0.048447333286726	-0.00182067141304808
-0.127651231082182	-0.111840341090044
0.256996780929455	-0.0119570379697445
0.792592842872745	0.581634000859109
0.533170244143429	0.770131860164237
6.992371732989937e-04	0.223697454824697
-0.0416767924640835	-0.0721671613011585
0.030120910923006	0.008629432692828
0.007063881864474	0.022919791706262

TABLE V

FILTER COEFFICIENTS WITH LENGTH 12 AND VANISHING MOMENT 4 DESIGNED BY l_1 NORM

h_0	g_0
0.019660953491772	0.005979749053996
0.036872657072564	0.034572185640262
-0.013057772609847	0.014753684202904
0.145920889738894	0.011155758186297
0.652405799239501	0.390261068273897
0.704226352135325	0.789405451872293
0.090621780240148	0.424670939341782
-0.209645338659644	-0.143871375304897
-0.045390840545540	-0.145806578467158
0.0312619618609236	0.018827811759382
0.002866861370513	0.017247918781127
-0.001529740961514	-0.002983050966790

TABLE VI
 FILTER COEFFICIENTS WITH LENGTH 12 AND VANISHING MOMENT
 3 DESIGNED BY l_1 NORM

h_0	g_0
0.00184807508959416	-0.000330561407625855
0.0220242771710574	0.0111727200722846
-0.0392361517965246	0.0131425880952590
-0.189542114839093	-0.128014156561420
0.102050660942876	-0.129120728397650
0.719196501572041	0.438201769576917
0.643493577302726	0.797167311190643
0.119314868728622	0.365883340298733
-0.0142880986540894	-0.00356154745295836
0.0365280289628551	0.0177028622275966
0.0132387183019659	0.0298097191588802
-0.000414780408934431	0.00216024557243620

TABLE VII
 E_1 AND E_2 OF DIFFERENT WAVELET BASES

The Filter	length	vanishing moment	E_1	E_2
Table I Designed by l_1 Norm	8	2	0.0048	4.6314E-5
Table I in [6]	8	3,2	0.0118	1.1267E-4
Table II Designed by l_∞ Norm	8	2	0.0127	1.4075E-4
Table III Designed by l_2 Norm	8	2	0.0291	6.8593E-4
Table IV Designed by l_1 Norm	10	3	0.0030	1.3949E-5
Table II in [6]	10	4,3	0.0121	2.081E-4
Example 2 in [4]	10	3	0.0215	6.0204E-4
Table V Designed by l_1 Norm	12	4	0.0020	5.4010E-6
Table III-A in [6]	12	5,4	0.0025	5.951E-5
Example 1 in [5]	12	4	0.0163	3.5389E-4
Table VI Designed by l_1 Norm	12	3	0.0013	2.6570E-6
Table III-B in [6]	12	4,3	0.0027	6.959E-6
Example 2 in [5]	12	3	0.0069	4.9798E-5